THE JOURNAL OF PHYSICAL CHEMISTRY B

ARTICLE

pubs.acs.org/JPCB

Density Functional Theory Investigations on the Structure and Dissolution Mechanisms for Cellobiose and Xylan in an Ionic Liquid: Gas Phase and Cluster Calculations

Rajdeep Singh Payal, R. Bharath, Ganga Periyasamy, and S. Balasubramanian*

Chemistry and Physics of Materials Unit, Jawaharlal Nehru Centre for Advance Scientific Research, Jakkur, Bangalore 560064, India

Supporting Information

ABSTRACT: Density functional theory (DFT) calculations have been carried out for cellobiose and xylan chosen as models for cellulose and hemicellulose, respectively, in gas phase, implicit and explicit solvent (water, methanol, and the ionic liquid, 1,3-dimethylimidazolium acetate) media using plane wave and atom centered basis set approaches in order to find out lowest energy conformers and configurations. Geometry, vibrational properties, and ^{1}H and ^{13}C NMR chemical shift values have been discussed under all three conditions. Calculations predict that inter- and intramolecular hydrogen bonding play an important role in the dissolution processes. In the gas phase and in implicit solvent, the anti−anti conformer of cellobiose and the anti−syn conformer of xylan are the most stable due to the formation of a large number of intramolecular hydrogen bonds. However, in the cluster calculations containing ion pairs of the ionic liquid (IL) surrounding the cellulosic units, the anti−syn conformer of cellobiose is more stable as intramolecular hydrogen bonds are substituted by intermolecular ones formed with the ions of the IL. The complexes of cellobiose (or of xylan) with the ions of the ionic liquid are stable with large negative binding energies ranging between −21 and −55 kcal mol^{-1}. The predicted ^{1}H NMR values of the lowest energy cellobiose conformers are in good agreement with the experimental value. Xylan binds stronger with the IL than cellobiose does by 20 kcal mol^{-1}. Furthermore, the two pentose rings in xylan are rotated by 60° to each other in contrast to their coplanarity in cellobiose, which can explain the higher solubility and the amorphous nature of hemicellulose in ionic liquids. The fewer number of hydroxyl groups in xylan (relative to cellobiose) does not affect the number of cations present in its first solvation shell while the number of anions is reduced.

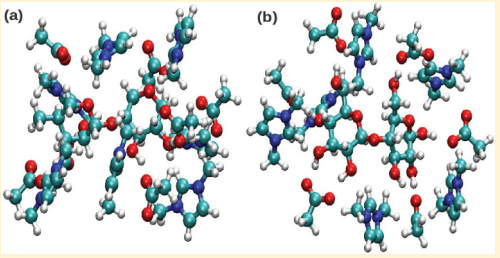

1. INTRODUCTION

Shrinking fossil fuel resources and environmental crises are major problems in the present world, which necessitate us to re-evaluate the efficient utilization of energy sources and find eco-friendly alternatives, such as, biorenewables.[1−3] Lignocellulosic material which is most abundant in wood/plant biomass is an example of such a resource. It chiefly contains lignin (20−30%), cellulose (40−50%), and hemicelluloses (20−30%).[4−6] Dissolving these organic polymers and breaking them into intermediate compounds that can be converted to biofuel (ethanol)/artificial silk remains a difficult task. Till now, only 40% of the ethanol content available in cellulosic feedstock is extracted effectively.[3]

Cellulose and hemicellulose are polysaccharides, present in plant cell wall with β-(1→4) linked backbones in an equatorial configuration.[7−9] Although both are polysaccharides, cellulose is a crystalline polymer with a highly ordered structure whereas hemicellulose is amorphous with a random structure, and many of them contains xylan backbone. In cellulose, cellobiose units are connected to one another via strong inter- and intramolecular hydrogen bonding networks (see Figure 1a) thus providing it and the cell wall with high chemical and mechanical stability. However, amorphous hemicellulose stabilizes the cell wall by interacting with neighboring hemicellulose, cellulose, or lignin units (Figure 1b).

Many research groups have tried to dissolve lignocellulosic material in common organic solvents at various physical conditions.[9−16] Some of the solvents such as *N*-methylmorpholine-*N*-oxide monohydrate, *N*,*N*-dimethylacetamide/LiCl, and $LiClO_4 \cdot 3H_2O$ have been shown to dissolve cellulose up to 15−20% of weight of lignocellulosic biomass. However, these solvents have disadvantages such as toxicity, instability, or high cost.[9−17] To overcome these issues, Rogers et al.[18] used room temperature ionic liquids (RTIL) as a solvent to dissolve cellulose. These ionic liquids are organic salts that have low melting temperatures (<100 °C) and negligible vapor pressure.[19−23] It has been reported that salts belonging to the dialkylimidazolium family (see Table 1) such as 1-*n*-butyl-3-methylimidazolium chloride ([C_4mim][Cl]) can dissolve cellulose and other polysaccharides in high concentrations with no derivatization at high temperature.[24] In addition, hemicellulose has also been dissolved in ionic liquids.[17] The solubility of cellulose and hemicellulose in various ionic liquids

Received: August 19, 2011
Revised: December 15, 2011
Published: December 15, 2011

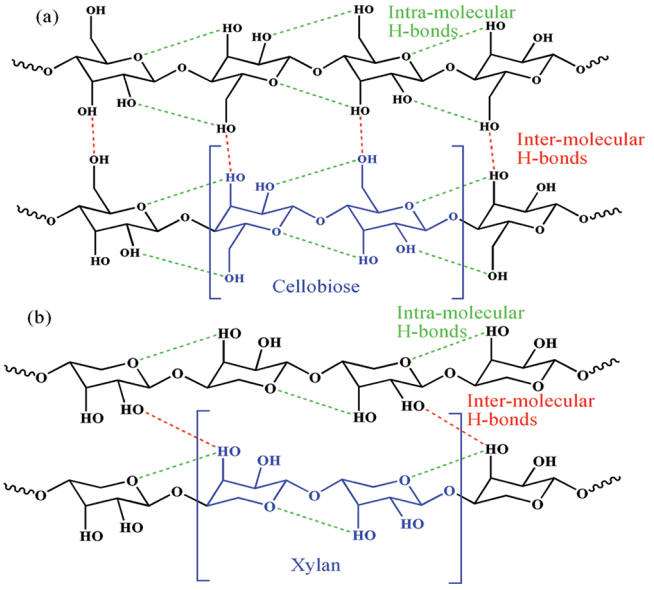

Figure 1. Schematic representation of (a) cellulose and (b) hemicellulose. In this article, monomer units of cellobiose and xylan are considered as representations of cellulose and hemicellulose (shown in blue color). Inter- and intramolecular hydrogen bonds are also shown.

Table 1. Various Ionic Liquids and Their Corresponding Cellulose and Hemicellulose Solubility at Room Temperature[a]

ionic liquid	cellulose solubility (wt %)	hemicellulose solubility (wt %)
$[C_4mim][CH_3COO]$	15.5−20.5[25,26]	10.0[17]
$[C_4mim][HSCH_2COO]$	13.5[27,28]	
$[C_4mim][HCOO]$	12.5[29]	
$[C_4mim][(C_6H_5)COO]$	12.0[28]	
$[C_4mim][H_2NCH_2COO]$	10.5[28]	
$[C_4mim][CH_3CHOHCOO]$	9.5[28]	

[a] Here C_4mim = 1-methyl,3-*n*-butylimidazolium cation.

at room temperature as reported by experimental groups are shown in the Table 1.

The ionic liquid with imidazolium cation and acetate anion has shown good wood solubility (15−20.5%) at room temperature.[30−32] Although it is now known that ionic liquids are suitable solvents of cellulose and hemicellulose, the mechanisms of dissolution of cellulose/hemicellulose in ionic liquids continues to be a matter of study.[1,33−39] Theoretical efforts are certainly poised to offer deep insights into the process of dissolution.

Gas phase, quantum chemical calculations on cellobiose[40] interacting with one ion pair[41,42] or only with cations or anions[43,44] have been reported. Also, classical molecular dynamics simulations of cellulose soaked in ionic liquids have also been previously reported.[45,46] However, quantum chemical computations in the presence of implicit and explicit solvent (IL) environments have not yet been reported, to our knowledge. This is one of the objectives of the current study. In addition, the dissolution of hemicellulose in ionic liquids has not been studied through computational methods. We believe that a comparison between cellulose and

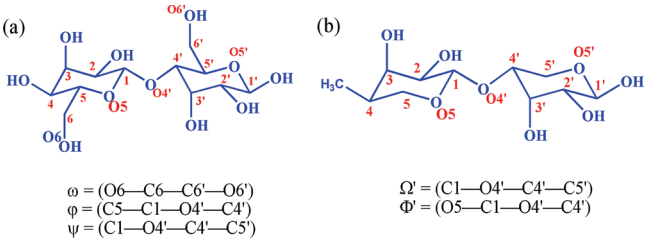

Figure 2. Schematic representation of (a) cellobiose and (b) xylan structures are shown. The numbering scheme and the dihedrals considered for the work are also shown.

hemicellulose can shed light on the role of hydroxyl group in their dissolution in ionic liquids. This approach is not only feasible but can also provide an understanding on the polarization and H-bonding interactions between solutes and ionic liquids. Insights obtained thus on the structural and electronic factors contributing to dissolution can be helpful to further increase the solubility of cellulose and hemicellulose in selected ionic liquids. It is important to note that cellobiose and xylan are simple carbohydrates and their derivatives have been already synthesized in the laboratory.[47,48]

The current study focuses on obtaining various ground state conformers (and configurations) of cellobiose and xylan in the gas phase, and in implicit and explicit IL solvent media. The lowest energy structures are validated by comparing the computed ^1H, ^{13}C NMR chemical shielding values with corresponding experimental data.[49,50] In what follows, section 2 is devoted to computational details. Various conformers of cellobiose and xylan are discussed in section 3. While section 4 describes the polarization on both the molecules due to the macroscopic dielectric constant of the solvent, section 5 explains the structural changes due to explicit IL solvation through cluster calculations. Conclusions are summarized in section 6.

2. COMPUTATIONAL DETAILS

Cellobiose (Figure 2a) and xylan (Figure 2b) are considered as models for cellulose and hemicellulose, respectively. There are many chiral centers in cellobiose and xylan, which leads to many conformers. Herein, the conformers of cellobiose were considered based on three important dihedral angles, which are: ω (O6−C6−C6′−O6′), φ (C5−C1−O4′−C4′) and ψ (C1−O4′−C4′−C5′). Similarly, the dihedral angles Ω' (C1−O4′−C4′−C5′) and Φ' (O5−C1−O4′−C4′) were considered for xylan. All the dihedral angles were varied from 0° to 180° in steps of 10° to identify the minimum energy structures.

The use of atom centered basis functions together with diffused and polarized basis sets for all atoms and hybrid functional has been well established for these kinds of systems.[51−55] However, this approach becomes increasingly expensive because of the computation of the multicenter electron integrals. We found it more computationally efficient to resort to a plane wave expansion combined with pseudopotentials, as implemented in, for example, the *ab initio* molecular dynamics package, CPMD.[56] Hence, some of the initial geometry optimizations were carried out using this code. Thus, the plane wave code[56] was used to screen structures and the final optimizations were carried out using the Gaussian code.[57] In the former calculations, the Perdew−Burke−Ernzerhof (PBE) exchange-correlation functional[58] was

dx.doi.org/10.1021/jp207989w |*J. Phys. Chem. B* 2012, 116, 833–840

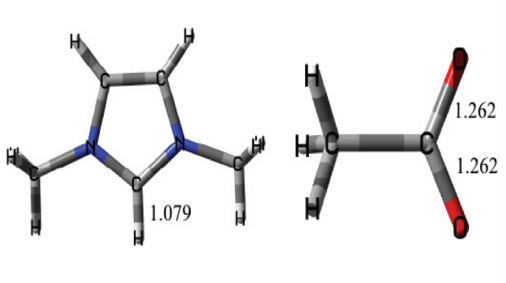

Figure 3. Optimized structures of $[C_1mim]^+$ and $[OAc]^-$ ions with important bond distances (Å) are shown.

employed with an energy cutoff for the wave function of 85 Ry. The effect of core electrons and the nuclei on the valence electrons were treated using Troullier−Martins pseudopotentials.[59] The optimizations were performed with tight energy convergence criterion and the maximum magnitude of the force on any ion was demanded to be less than 10^{-5} a.u. The optimizations were carried out in a cubic box of edge length 16.0 Å. Cluster boundary conditions[60] and the Hockney−Poisson solver consistent with calculations for an isolated system were employed. The four lowest energy conformers found in the plane wave approach were further optimized using B3LYP hybrid exchange[61−63] and correlation functional with 6-31++G(d, p) atomic center basis set as implemented in the *Gaussian 03* program.[57] It is noteworthy that the energy ranking of these structures as obtained from the PBE/85 Ry and the B3LYP/6-31++G(d, p) calculations matched. Similar methods have been adopted by other workers in the quantum modeling of ion pairs of ionic liquids and systems similar to those studied here.[22,64−66] Local properties of the system, such as NMR chemical shielding values and local atomic charges were calculated using the Gaussian code. The optimized structures in gas phase and implicit solvation media were characterized as minima on the basis of calculation of their harmonic vibrational frequencies and no imaginary frequencies were observed. All the results reported here were obtained from the B3LYP/6-31++G(d, p) set of calculations.

Although both implicit and explicit solvation media were considered for cellobiose in order to understand the effect of three solvents—water, methanol, and ionic liquid—the calculations for xylan under explicit solvent conditions were carried out only with the ionic liquid. Implicit solvent calculations were carried out using the polarized continuum model (PCM) approach as implemented in the *Gaussian 03* program. This provides the effect of electrostatic interactions alone on the solubility of molecules. In these calculations, the dielectric constants of water, methanol, and the ionic liquid were taken as 80, 33, and 11, respectively. The effect due to hydrogen bonding (and any other specific) interaction between the solvent molecules and the cellobiose unit was also studied by explicitly surrounding the cellobiose unit with layer(s) of solvent molecules. Initially, various configurations of solvent molecules around the lowest energy gas phase conformers of cellobiose and xylan were studied using plane wave approach as the CPMD code scaled well. Four low energy configurations were further optimized in the atom centered basis set approach. The detail of number of configuration studied in gas, implicit and explicit solvent media for both molecules are explained in the Supporting Information. Although in the case of water and methanol 19 molecules were considered to form the solvent layer, for the case of the ionic liquid, seven

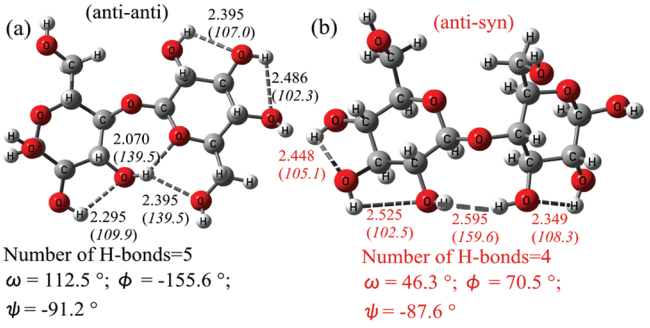

Figure 4. Computed two lowest energy conformers of cellobiose in the gas phase. Hydrogen bonds are shown as dotted lines and their lengths (Å) and angles (degrees) are indicated. Important dihedral angles (degrees) are also shown.

Table 2. Computed Energy Differences (ΔE) between the Most Stable Conformers in Gas and Implict Solvent Media[a]

molecules	medium		ΔE (kcal mol^{-1})	
			anti−anti	anti−syn
cellobiose	gas phase		0.0	4.53
	implicit solvent	IL	0.0	1.97
		water	0.0	1.60
		methanol	0.0	1.27
			anti−syn (conformer 2)	anti−syn (conformer 1)
xylan	gas phase		0.0	3.22
	implicit solvent	IL	0.0	2.53
		water	0.0	1.40
		methanol	0.0	2.68

[a] All energies include contributions from zero-point energy correction (ZPE).

molecules of ($[C_1mim][OAc]$) were explicitly considered to surround the cellobiose unit. As mentioned earlier, calculations with explicit solvent molecules for xylan were carried out only with the ionic liquid. Here again, seven ion pairs were included. The number of ion pairs was chosen based on the reported experimental NMR studies.[49] Such cluster calculations, mimicking the effect of the solvent have been carried out for other systems.[67] All the molecular properties were calculated at the same level of theory and using the *Gaussian 03* program package. ^1H and ^{13}C NMR chemical shielding values were calculated using the gauge including atomic orbital (GIAO) method.[68−72] The molecular structure of a cation and an anion are shown in Figure 3. Coordinates of geometry optimized molecules and complexes are provided in the Supporting Information.

3. RESULTS AND DISCUSSION

3.1. Low Energy Conformers of Cellobiose in the Gas Phase. Density functional theory based computations have been carried out to identify low energy conformers of cellobiose in the gas phase. Among the various structures, the anti−anti and anti−syn conformers are highly stable with the maximum number of intramolecular H bonds (see Figure 4). The presence of an additional H-bond stabilizes the anti−anti conformer by 4.53 kcal mol^{-1} (Table 2) relative to the anti−syn one.

Table 3. Computed −OH IR Stretching Frequency (cm^{-1}) for Two Lowest Energy Conformers of Cellobiose (Figure 4) and Xylan (Figure 5)

			IR frequency (cm^{-1})	
molecules	media		free OH	H-bonded
cellobiose	gas phase	anti−anti	3845−3850	3721−3826
		anti−syn	3746−3818	3691−3712
	implicit IL	anti−anti	3495−3630	3414−3478
		anti−syn	3557−3581	3537−3555
xylan	gas phase	conformer 1	3810−3840	3790−3807
		conformer 2	3835−3850	3770−3830
	implicit IL	conformer 1	3810−3840	3780−3820
		conformer 2	3810−3860	3760−3800

The presence and the strength of H bonds red shifts the −OH (covalent bond) stretching frequency when compared with that for free −OH (i.e., −OH without the H-bonding interaction) in the same molecule. For example, in the anti−anti conformer, three different −OH stretching frequencies were observed: 3721 cm^{-1} (for O3′-H3′), 3785−3826 cm^{-1} (for O2−H2, O2′−H2′, O3−H3, O1′−H1′) and 3845−3850 cm^{-1} (O6−H6, O6′−H6′, O4−H4) (See Table 3). These are consistent with the magnitude of the H-bond strength of the OH donors, which are O3′−H3′ > O2−H2 ≈ O2′−H2′ ≈ O3−H3 ≈ O1′−H1′ > O6−H6 ≈ O6′−H6′ ≈ O4−H4 and also reflected in the bond distances as shown in Figure 4. Similarly, two types of −OH stretching modes were observed for the anti−syn conformer with respect to their H-bond formation ability.

Room temperature ^{1}H and ^{13}C NMR data of synthetic cellobiose analogues and of [C_2mim][OAc] have been reported in DMSO-d6 solvent at different mole fractions.[49,50] However, chemical shift values were discussed only for specific atoms due to experimental difficulties. It would thus be useful for us to validate our computational work against these experimental data. The calculated ^{1}H NMR chemical shift values of 2−5 ppm for the H-bonded −OH and ^{13}C NMR values 55−95 ppm for the anti−anti conformer are comparable to the experimental ^{1}H (3−5 ppm) and ^{13}C NMR values (49−91 ppm) of cellobiose synthetic analogues. In contrast, the corresponding values for the anti−syn conformer are ^{1}H, 1.5−2.5 ppm and ^{13}C, 52−90 ppm (see Table S1 of the Supporting Information).[47,73] Minor differences in the chemical shift value are likely due to differences in the functional groups between the synthetic analogues and cellobiose and also due to the absence of a solvent environment in these calculations. The presence of one extra H-bond in anti−anti conformer (O3′−H3′···O6) shifted the H3′ ^{1}H NMR value to the downfield (4.65 ppm) than in the anti−syn conformer (2.07 ppm). Furthermore, the computed energy difference of 4.53 kcal mol^{-1} between the anti−anti and anti−syn conformers at the B3LYP/6-31++G(d, p) level is in good agreement with the value of 5 kcal mol^{-1} as reported through MP2/6-31G(d) calculations in the gas phase.[43] These data further validate the methods adopted here.

3.2. Gas Phase Structure of Xylan. The lowest energy conformers for xylan are analyzed based on the Ω′ and Φ′ dihedral angles. In contrast to cellobiose, the two pentose rings in xylan are oriented at 70° to each other. This prevents the formation of a large number of intramolecular H bonds as in cellobiose. The anti−syn conformers 1 and 2 (shown in Figure 5) are lower in energy than the others (anti−anti and syn-syn). The anti−syn conformers differ from each other in the orientation of the −OH groups, which leads to different number of intramolecular H bonds. The larger number of intramolecular H bonds in the anti−syn conformer C2 (panel b of Figure 5) stabilizes it by 3.22 kcal mol^{-1} (see Table 2) than conformer C1 (panel a of Figure 5). Similar to the case of cellobiose, the presence of H-bonding interactions is reflected in the −OH stretching frequencies and ^{1}H NMR values. The presence of both free (i.e., −OH group without any H bonding interaction) as well as H-bonded OH groups in the conformers leads to a large spread of OH stretching frequency ranging from 3770 cm^{-1} to 3820 cm^{-1} (see Table 3). This is also observed in the values of ^{1}H NMR chemical shift which is in the range of 1.87−2.28 ppm for the H-bonded OH group. Extra H-bond in anti−syn conformer 2 shifts the ^{1}H NMR value of the H2′ (1.27) atom to downfield more than the anti−syn conformer 1 H2′ (0.79). Compared to the values for free OH, these are shifted downfield by 1.0−1.6 ppm. In addition, the structural differences between cellobiose and xylan are reflected in the ^{13}C NMR chemical shift values as shown in Table S1.

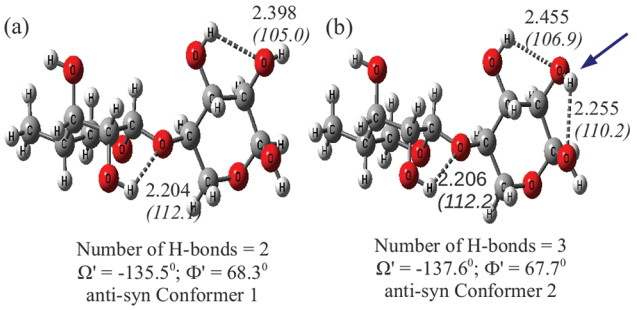

Number of H-bonds = 2
Ω' = -135.5⁰; Φ' = 68.3⁰
anti-syn Conformer 1

Number of H-bonds = 3
Ω' = -137.6⁰; Φ' = 67.7⁰
anti-syn Conformer 2

Figure 5. Computed two lowest energy conformers of xylan in the gas phase. Important dihedral angles (degrees) and bond distances (Å) are shown. Note the difference in the orientation of the two pental rings in either of these conformers, as compared to that in cellobiose. Note also the orientation of the O−H bond (indicated by an arrow) in conformer 2 leading to the formation of an additional hydrogen bond.

4. IMPLICIT SOLVATION

While gas phase calculations provide details of the structure and hydrogen bonding in the cellulosic units, it will be more appropriate to compare experimental data to a system in which such units are solvated at the same thermodynamic conditions as in experiments. With advancements in simulation methods and computing environments, this is an achievable aim to a large extent through the method of *ab initio* molecular dynamics simulations. Pending such simulations which we plan to carry out in future, in the current work we have studied the effect of solvation of cellulosic units through two "gas phase" quantum techniques: (i) using a dielectric continuum model and (ii) cluster calculations of cellulosic units surrounded by layer(s) of solvent molecules. In this section, we discuss results of the former.

4.1. Implicit Solvation Effects on Cellobiose. Four lowest energy conformers of cellobiose obtained from plane wave calculations in the gas phase were further optimized within dielectric media using the atom centered basis set approach (*Gaussian 03*).[57] The inclusion of the dielectric medium did not affect the order of the stability of the conformers. However, it reduced the energy difference between the stable conformers (see Figures 4 and 5 for the gas phase structures) by 2.56 kcal mol^{-1} (IL), 2.93 kcal mol^{-1}

dx.doi.org/10.1021/jp207989w |J. Phys. Chem. B 2012, 116, 833–840

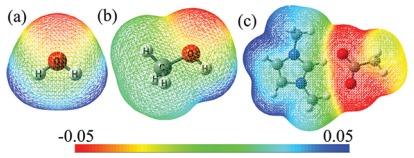

Figure 6. Mapping of the molecular electrostatic potential (MEP) on an isocontour of the electron density taken to be 0.04 e bohr^{-3} for (a) water, (b) methanol, and (c) an ion pair, [C_1mim][OAc].

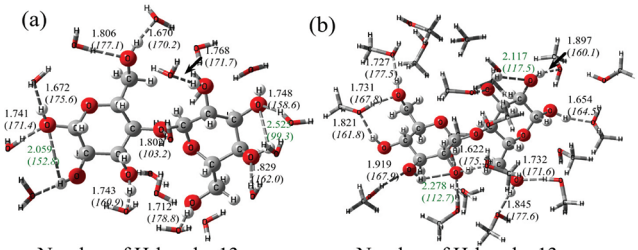

Figure 7. Computed lowest energy configurations of cellobiose in (a) water and (b) methanol clusters. Nine inter- and four intramolecular hydrogen bonds are seen. Various structural parameters are also shown.

(water), and 3.02 kcal mol^{-1} (methanol) (see Table 2). Increasing the dielectric constant decreases the energy difference between the anti−anti and anti−syn conformer by the following amounts: for IL (1.97 kcal mol^{-1}), methanol (1.60 kcal mol^{-1}), and for water (1.27 kcal mol^{-1}). The hydrogen bond length is seen to correspondingly increase by 0.01−0.03 Å. The subtle change in the interaction strength is also reflected in the −OH stretching mode and in the ^{1}H NMR chemical shielding values (see Tables 3 and S1). The −OH stretching mode of anti−anti cellobiose in IL is red-shifted by about 200 cm^{-1} relative to the gas phase value. Implicit solvation also changes the ^{1}H NMR chemical shift values of the hydroxyl group upfield by 0.2−0.4 ppm than in the gas phase due to the weakening of H bonds. The computed ^{1}H and ^{13}C NMR chemical shift values for the anti−anti conformer in the implicit solvation media are in good agreement with experimental values. This provides further evidence for the stability of the anti−anti conformer of cellobiose molecule.

4.2. Implicit Solvation Effect on Xylan. Similar to cellobiose, implicit solvation did not affect the conformer stability order of xylan. However, the energy difference between the two conformers was reduced by 0.69 kcal mol^{-1} in the implicit presence of the ionic liquid. For both conformers of xylan, the H-bonded −OH stretching frequencies were red-shifted (3780−3830 cm^{-1} for conformer 1 and 3760−3800 cm^{-1} for conformer 2) than for the free −OH group (3810−3840 cm^{-1} for conformer 1 and 3810−3860 cm^{-1} for conformer 2) (see Table 3). The polarization effects due to intramolecular H bonds are also clearly reflected in the ^{1}H NMR (2.91−3.74 ppm) and ^{13}C NMR (41.93−105.04 ppm) chemical shielding values, which is shifted upfield by 0.8−2.9 ppm compared with their gas phase values (see Table S1).

The implicit solvations studies suggest that a solvent with high polarization could dilute intermolecular H bonds of cellobiose and xylan. To verify this, calculations with explicit solvent molecules need to be carried out. This is the object of the next section.

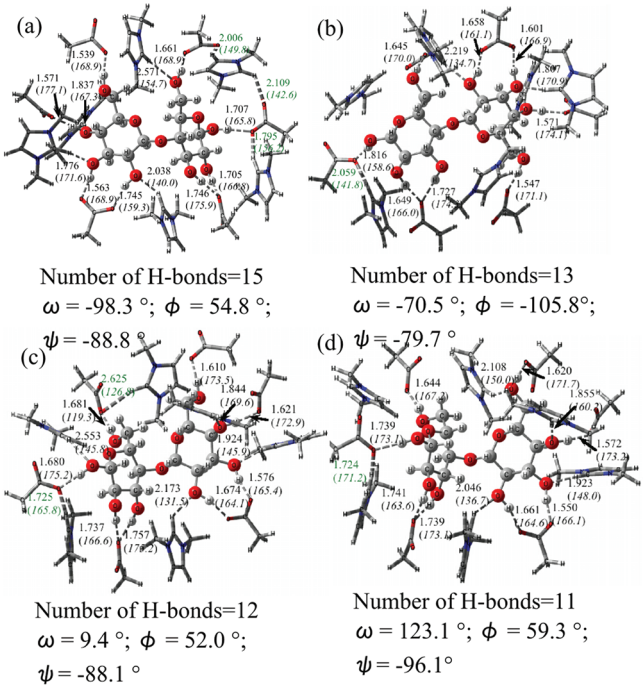

Figure 8. Computed lowest energy configurations of cellobiose surrounded by ion pairs of [C_1mim][OAc] ionic liquid. Intermolecular H bonds between cellobiose and the ions as well as relevant structural parameters are shown.

5. EXPLICIT SOLVATION EFFECTS

An understanding of explicit solvent effects on the energetics and structure of cellobiose and xylan units requires an appreciation of the electrostatics of the molecules involved. Compared with water (oxygen: −0.720 e; hydrogen: 0.36 e) and methanol (oxygen: −0.541 e, hydrogen: 0.340 e), the acetate oxygen (−0.751 e) and the acidic hydrogen of the imidazolium cation (0.527 e) have high negative and positive Mulliken atomic charges respectively. This suggests the higher ability of IL to donate or accept H bonds relative to water or methanol. The difference in charge density between the three solvents is clearly seen in the molecular electrostatic potential maps too (Figure 6).

5.1. Explicit Solvation Effects: Cellobiose. The computed lowest energy conformers in the gas phase for cellobiose were also optimized in the presence of explicit solvent environment. A layer of solvent molecules were added at arbitrary locations around the cellobiose molecule, as an initial configuration for geometry optimization runs.

In the optimized configuration, water and methanol molecules form intermolecular H bonds with cellobiose as shown in Figure 7. However, this solvation does not completely break the intramolecular H-bonding between cellobiose moieties. The calculated negative BE values ranging between −10 and −20 kcal mol^{-1} reflect the stability of water/methanol solvated cellobiose cluster. The anti−anti conformer is highly stable in both water and methanol media than the anti−syn conformer, similar to its stability in the gas and implicit solvent phases. We notice that the small size of the water/methanol molecules allows for all the nineteen solvent molecules to be present in the first coordination shell of cellobiose. Further, intermolecular H-bonding is seen to weaken the intramolecular H bonds, which can decrease the energy

dx.doi.org/10.1021/jp207989w |J. Phys. Chem. B 2012, 116, 833–840

Table 4. Computed Energy Differences (ΔE) between the Most Stable Configurations in Explicit IL Solvent Medium[a]

molecules	IL clusters	ΔE (kcal mol^{-1})	binding energy (kcal mol^{-1})
cellobiose	configuration 1 (anti−syn conformer)	0.0	−21.10
	configuration 2 (anti−anti conformer)	6.02	−11.05
	configuration 3 (anti−syn conformer)	11.22	−9.98
	configuration 4 (anti−syn conformer)	13.13	−8.07
xylan	configuration 1 (anti−syn conformer 1)	0.0	−55.39
	configuration 2 (anti−syn conformer 2)	16.52	−35.26

[a] Binding energy (BE) = $E_{\text{IL-cellobiose/xylan cluster}} - (E_{\text{cellobiose/xylan}} + NE_{\text{IL pairs}})$, where N denotes the number of solvent ion pairs ($N = 7$). Note that the ZPE corrections are not included in the ΔE, BE values.

difference between the anti−anti and anti−syn conformers by 0.2−0.3 kcal mol^{-1} (see Table S2).

However, the effect on cellobiose due to the explicit solvation by ion pairs of an IL is vastly different. In particular, the larger size of the cation and the anion prevents the direct, proximal interaction between every ion and the −OH group of cellobiose. This is clearly reflected in the computed minimum energy geometries of cellobiose which are shown in Figure 8.

Optimization of cellobiose solvated by ion pairs of [C_1mim][OAc] leads to four low energy configurations, where the cellobiose unit is present in anti−syn configuration 1 (Figure 8a), anti−anti configuration 2 (Figure 8b), anti−syn configuration 3 (Figure 8c), and anti−syn configuration 4 (Figure 8d). All four configurations have negative binding energies ranging from −8.07 to −21 kcal mol^{-1} (see Table 4), which indicates the strong interaction between the ions and cellobiose. The computed BE values in "IL medium" is larger than the corresponding values for water and methanol media. The high H-donating and accepting nature of ion pairs results in the formation of strong intermolecular H bonds and also breaks all the intramolecular H bonds of cellobiose.

Dramatically, these effects swap the order of conformer stability. In the presence of [C_1mim][OAc], the anti−syn configuration becomes more stable than the anti−anti conformer by 6 kcal mol^{-1} (see Tables 2 and 4). This is in contrast to the observations on conformer stability found in the gas, implicit solvent, explicit water, and methanol media. Furthermore, in agreement with NMR studies,[49,50] both the cation and the anion of the IL are seen to interact with the cellobiose unit. All the seven anions form strong H bonds with the cellobiose solute. However among the seven cations, only four form H bonds with cellobiose. The remaining cations form H bonds with the anions alone. Values of dihedral angles for the four lowest energy conformers studied here are in good agreement with those seen in molecular dynamics simulations. The values seen in MD simulations were ($\varphi = -125°$, $\psi = 50°$), ($\varphi = -50°$, $\psi = 100°$), and ($\varphi = -120°$, $\psi = -50°$).[46] The changes from intra- to intermolecular H-bonding network are also clearly reflected in the ^{1}H NMR values of the hydroxyl group as shown in Table S1 of the Supporting Information. Strong intermolecular H-bonding interactions are the reason for larger downfield movement of ^{1}H and ^{13}C chemical shifts by 3.5−4.6 ppm and 66.5−80.1 ppm compared to the values observed in gas and implicit solvent media calculations. The computed chemical shift values are comparable with experimental ^{1}H (3.0−6.0 ppm) and ^{13}C (68.0−103.0 ppm) NMR chemical shift values.[49,50] Minor differences could be due to the lack of more solvent layers in the calculations. In the next section, we examine the stability of conformers of xylan in the explicit IL medium.

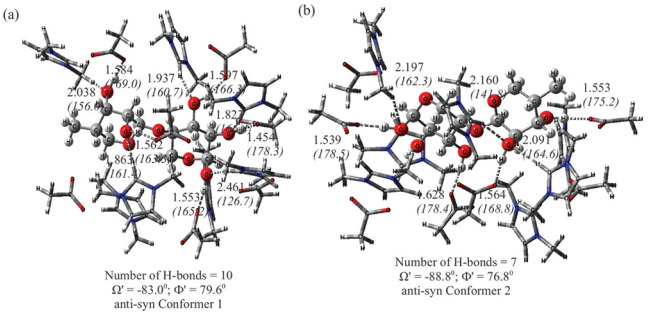

Figure 9. Computed lowest energy structures of xylan in the IL solvent medium. Intermolecular H bonds between xylan and ion pairs and relevant structural parameters are shown.

5.2. Explicit Solvation Effects on Xylan. Similar to cellobiose, xylan forms intermolecular H-bonding with ions which leads to negative binding energy values of −33 to −51 kcal mol^{-1}. The computed binding energy for xylan is higher by −29 kcal mol^{-1} than that for the cellobiose molecule, which is a likely reason for the high solubility of hemicellulose in IL media over that of cellulose.[17] Figure 9 shows two of the low energy configurations of xylan "solvated" by ions of the ionic liquid. Again, conformer 2 (Figure 9b) differs from conformer 1 (Figure 9a) in the orientation of the OH group indicated by an arrow in Figure 5. Similar to cellobiose, the xylan molecule also interacts with four cations. This shows that the fewer number of hydroxyl groups on xylan does not affect its interactions with the cation. However the number of anions forming hydrogen bonds with xylan is reduced to a value of six from the value of seven that was observed for cellobiose. This difference could be a minor one and its importance (or otherwise) can be checked only by doing simulations of the solute in explicit bulk solvent. Further, six out of seven anions of the IL form H bonds with xylan. The intermolecular H bonds between the ions and xylan are shorter by 0.1−0.3 Å than the corresponding distances between the ions and cellobiose., There are no intramolecular hydrogen bonds in both the configurations of solvated xylan. Configuration 1 contains ten intermolecular hydrogen bonds (i.e., xylan forming H bonds either with the cation or the anion) stabilizing it over configuration 2 in which only seven intermolecular H bonds are observed. The reduction in the number of H bonds in conformer 2 is due to the orientation of the −OH group indicated by an arrow in Figure 5. These results suggest that the cation in the IL could also be involved in the solvation by the formation of intermolecular H bonds with the cellulosic units, similar to those formed by the anion. In addition, the xylan molecules

maintain the 60° orientation between the pental rings as in gas phase, which might be the reason for its amorphous nature.

6. CONCLUSIONS

We have carried out quantum chemical calculations of cellobiose and xylan in order to obtain a microscopic understanding of their solubility in ionic liquids. The calculations, using density functional theory, have been performed in (a) gas phase, (b) under implicit solvent conditions, and (c) with a layer of explicit solvent molecules. The solvent molecules considered were water, methanol, and 1,3-dimethylimidazolium acetate, $[C_1mim][OAc]$.

Our study shows that the conformational stability of cellobiose and xylan are highly dependent upon the number of inter- and intramolecular H bonds. In the gas phase, the moiety with large number of intramolecular H bonds (the anti−anti conformer of cellobiose and the anti−syn conformer 2 of xylan) is most stable. The structural features were reflected in the calculated NMR chemical shifts and vibrational frequencies. The energy differences between the conformers are within 5−6 kcal mol^{-1} which is within the capability of the solvent to induce a conformational change. The polarization effect due to the dielectric constant of the solvent, captured through continuum calculations, is seen to further reduce the energy difference. The primary cause appears to be the reduction of the H-bond strength; however the conformers follow the same trend in energy as in the gas phase.

In addition, our quantum calculations on a cluster of solvent molecules solvating the cellulosic units yield rich information on solute−solvent hydrogen bonding.[74,75] While the explicit presence of water and methanol around cellobiose (or xylan) does not change the order of conformational stability, it is seen to partially remove the intramolecular H bonds. Strikingly, all intramolecular H bonds are removed in the explicit IL medium, due to strong solute−solvent H-bonding interaction. As a result, the anti−syn conformer of cellobiose and the anti−syn conformer 1 of xylan (wherein the glucose units are rotated by about 60°) become more stable than other conformers. Nearly all the anions coat (forming hydrogen bonds) cellobiose exclusively, while only a fraction of the cations do so. This result is in good agreement with experimental NMR studies.[49,50] The remaining cations form H bonds with their corresponding anions. The same trend was observed in xylan, where out of the seven ion pairs present in the calculation, four cations and six anions form strong solute−solvent hydrogen bonds. However, the two rings in xylan are oriented at 60° to each other, while in cellobiose they are coplanar.

The computed structural parameters of cellobiose−IL cluster, especially dihedral values are in good agreement with those seen in earlier molecular dynamics simulations.[46] Our studies suggest that both the cation and the anion are responsible for the dissolution of cellobiose and xylan in ionic liquids, which is in good agreement with previous experimental studies.[49,50] In addition, our results confirm that the H-bonding interactions between anion and cation with the cellobiose or xylan units contribute significantly in their dissolution. The work also points out the necessity of considering explicit solvent molecules to capture these subtle effects that are so crucial to cellulose solubility in room temperature ionic liquids.

■ ASSOCIATED CONTENT

Ⓢ Supporting Information. Computational details, computed ^1H and ^{13}C NMR values of cellobiose and xylan molecules in various environments, and the energetics of the cellobiose−methanol and cellobiose−water clusters. Also provided are coordinates of optimized configurations. This material is available free of charge via the Internet at http://pubs.acs.org.

■ AUTHOR INFORMATION

Corresponding Author
*E-mail: bala@jncasr.ac.in.

■ ACKNOWLEDGMENT

We thank the Department of Science and Technology for support. G.P. thanks DST-Women Scientists Fellowship for funding.

■ REFERENCES

(1) Simmons, B. A.; Loque, D.; Blanch, H. W. *Genome Biol.* **2008**, *9*, 242.
(2) Wynman, C. E. *Trends Biotechnol.* **2007**, *25*, 153–157.
(3) Richard, T. L. *Science* **2010**, *329*, 793–796.
(4) Saha, B. C. *J. Ind. Microbiol. Biotechnol.* **2003**, *30*, 279–291.
(5) Ohno, H.; Fukaya, Y. *Chem. Lett.* **2009**, *38*, 2–7.
(6) Kennedy, J. F.; Phillips, G. O.; Williams, P. A. *Cellulose sources and exploitation: industrial utilization, biotechnology, and physico-chemical properties*; Ellis Horwood Ltd.: New York, 1990.
(7) Scheller, H. V.; Ulvskov, P. *Annu. Rev. Plant. Biol.* **2010**, *61*, 263–289.
(8) Pinkert, A.; Marsh, K. N.; Pang, S.; Staiger, M. P. *Chem. Rev.* **2009**, *109*, 6712–6728.
(9) Nishino, T.; Matsuda, I.; Hirao, K. *Macromolecules* **2004**, *37*, 7683–7687.
(10) Terbojevich, M.; Cosani, A.; Conio, G.; Ciferri, A.; Bianchi, E. *Macromolecules* **1985**, *18*, 640–646.
(11) Nishio, Y.; Manley, R. S. J. *Macromolecules* **1988**, *21*, 1270–1277.
(12) McCormick, C. L.; Dawsey, T. R. *Macromolecules* **1990**, *23*, 3606–3610.
(13) Williamson, S. L.; Armentrout, R. S.; Porter, R. S.; McCormick, C. L. *Macromolecules* **1998**, *31*, 8134–8141.
(14) Edgar, K. J.; Buchanan, C. M.; Debenham, J. S.; Rundquist, P. A.; Seiler, B. D.; Shelton, M. C.; Tindall, D. *Prog. Polym. Sci.* **2001**, *26*, 1605–1688.
(15) Kuang, Q. L.; Zhao, J. C.; Niu, Y. H.; Zhang, J.; Wang, Z. G. *J. Phys. Chem. B* **2008**, *112*, 10234–10240.
(16) Kubisa, P. *Prog. Polym. Sci.* **2009**, *34*, 1333–1347.
(17) Zhao, H.; Baker, G. A.; Cowins, J. W. *Biotechnol. Prog.* **2010**, 26.
(18) Swatloski, R. P.; Spear, S. K.; Holbrey, J. D.; Rogers, R. D. *J. Am. Chem. Soc.* **2002**, *124*, 4974–4975.
(19) Welton, T. *Chem. Rev.* **1999**, *99*, 2071–2084.
(20) Anderson, J. L.; Ding, J.; Welton, T.; Armstrong, D. W. *J. Am. Chem. Soc.* **2002**, *124*, 14247–14254.
(21) Ludwig, R. *ChemPhysChem* **2006**, *7*, 1415–1416.
(22) Bhargava, B. L.; Balasubramanian, S.; Klein, M. L. *Chem. Commun.* **2008**, *44*, 3339–3351.
(23) Maginn, E. J. *J. Phys., Condensed Matter* **2009**, *21*, 373101.
(24) Fort, D. A.; Swatloski, R. P.; Moyna, P.; Rogers, R. D.; Moyna, G. *Chem. Commun.* **2006**, 714–716.
(25) Zavrel, M.; Bross, D.; Funke, M.; Büchs, J.; Spiess, A. C. *Bioresour. Technol.* **2009**, *100*, 2580–2587.
(26) Singh, S.; Simmons, B. A.; Vogel, K. P. *Biotechnol. Bioeng.* **2009**, *104*, 68–75.
(27) Fukaya, Y.; Sugimoto, A.; Ohno, H. *Biomacromolecules* **2006**, *7*, 3295–3297.
(28) Airong, X.; Wang, J.; Wang, H. *Green Chem.* **2010**, *12*, 268–275.
(29) Fukaya, Y.; Hayashi, K.; Wadeb, M.; Ohno, H. *Green Chem.* **2008**, *10*, 44–46.
(30) Sun, N.; Rahman, M.; Qin, Y.; Maxim, M. L.; Rodríguez, H.; Rogers, R. D. *Green Chem.* **2009**, *11*, 646–655.

(31) Samayam, I. P.; Hanson, B. L.; Langan, P.; Schall, C. A. *Biomacromolecules* **2011**, *12*, 3091–3098.
(32) Lovell, C. S.; Walker, B. L.; Damion, R. A.; Radhi, A.; Tanner, S. F.; Budtova, T.; Ries, M. E. *Biomacromolecules* **2010**, *11*, 2927–2935.
(33) Mason, P. E.; Neilson, G. W.; Enderby, J. E.; Saboungi, M. L.; Brady, J. W. *J. Am. Chem. Soc.* **2005**, *127*, 10991–10998.
(34) Mason, P. E.; Neilson, G. W.; Enderby, J. E.; Saboungi, M. L.; Brady, J. W. *J. Phys. Chem. B* **2005**, *109*, 13104–13111.
(35) Remsing, R. C.; Swatloski, R. P.; Rogers, R. D.; Moyna, G. *Chem. Commun.* **2006**, 1271–1273.
(36) Youngs, T. G. A.; Hardacre, C.; Holbrey, J. D. *J. Phys. Chem. B* **2007**, *111*, 13765–13774.
(37) Remsing, R. C.; Hernandez, G.; Swatloski, R. P.; Massefski, W. W.; Rogers, R. D.; Moyna, G. *J. Phys. Chem. B* **2008**, *112*, 11071–11078.
(38) da Costa Sousa, L.; Chundawat, S. P. S; Balan, V.; Dale, B. E. *Curr. Opin. Biotechnol.* **2009**, *20*, 339–347.
(39) Peng, X.; Ren, J.; Sun, R. *Biomacromolecules* **2010**, *11*, 3519–3524.
(40) Bergenstable, M.; Wrhlert, J.; Himmet, M. E.; Brady, J. W. *Carbohydr. Res.* **2010**, *345*, 2060–2066.
(41) Jinxin, G.; Zhang, D.; Liu, C. *J. Theor. Comput. Chem.* **2010**, *9*, 611–624.
(42) Janesko, B. D. *Phys. Chem. Chem. Phys.* **2011**, *13*, 11393–11401.
(43) Mohamed, M. N. A.; Watts, H. D.; Guo, J.; Catchmark, J. M. *Carbohydr. Res.* **2010**, *345*, 1741–1751.
(44) Jinxin, G.; Zhang, D.; Duan, C.; Chengbu, L. *Carbohydr. Res.* **2010**, *345*, 2201–2205.
(45) Derecskei, B.; Derecskei-Kovacs, A. *Mol. Sim.* **2006**, *32*, 109–115.
(46) Liu, H.; Sale, K. L.; Holmes, B. M.; Simmons, B. A.; Singh, S. *J. Phys. Chem. B* **2010**, *114*, 4293–4301.
(47) Novoselov, N. P.; Sashina, E. S.; Petrenko, V. E.; Zaborsky, M. *Fibre Chem.* **2007**, *39*, 153–158.
(48) Binder, J. B.; Raines, R. T. *Proc. Natl. Acad. Sci.* **2010**, *107*, 4516–4521.
(49) Zhang, J.; Zhang, H.; Wu, J.; He, J.; Xiang, J. *Phys. Chem. Chem. Phys.* **2010**, *12*, 1941–1947.
(50) Hesse-Ertelt, S.; Heinze, T.; Kosan, B.; Schwikal, K.; Meister, F. *Macromol. Symp.* **2010**, *294*, 75–89.
(51) Appell, M.; Strati, G.; Willett, J. L.; Momany, F. A. *Carbohydr. Res.* **2004**, *339*, 537–551.
(52) Csonka, G. I.; French, A. D.; Johnson, G. P.; Stortz, C. A. *J. Chem. Theor. Comput.* **2009**, *5*, 679–692.
(53) Jockusch, R. A.; Talbot, F. O.; Rogers, P. S.; Simone, M. I.; Fleet, G. W. J.; Simons, J. P. *J. Am. Chem. Soc.* **2006**, *128*, 16771–16777.
(54) Kozmon, S.; Tvaroska, I. *Collect. Czech. Chem. C* **2006**, *71*, 1453–1469.
(55) Momany, F. A.; Appell, M.; Willett, J. L.; Bosma, W. B. *Carbohydr. Res.* **2005**, *340*, 1638–1655.
(56) Hutter, J.; Ballone, J. P.; Bernasconi, M.; Focher, P.; Fois, E.; Goedecker, S.; Marx, D.; Parrinello, M.; Tuckerman, M. E. *CPMD*; Max Planck Institut fuer Festkoerperforschung and IBM Zurich Research Laboratory: Stuttgart, 1990.
(57) Frisch, M. J.; et al. *Gaussian 03*, revision C.02; Gaussian Inc.: Wallingford, CT, 2004.
(58) Perdew, J. P.; Burke, K.; Ernzerhof, M. *Phys. Rev. Lett.* **1996**, *77*, 3865–3868.
(59) Troullier, N.; Martins, J. L. *Phys. Rev. B* **1991**, *43*, 1993.
(60) Barnett, R. N.; Landman, U. *Phys. Rev. B* **1993**, *48*, 2081–2097.
(61) Becke, A. D. *J. Chem. Phys.* **1993**, *98*, 5648–5652.
(62) Lee, C.; Yang, W.; Parr, R. G. *Phys. Rev. B* **1988**, *37*, 785–789.
(63) Parr, R. G.; Wang, W. *Density-Functional Theory of Atoms and Molecules*; Oxford University Press: New York, 1989.
(64) Zahn, S.; Bruns, G.; Thar, J.; Kirchner, B. *Phys. Chem. Chem. Phys.* **2008**, *10*, 6909–7048.
(65) Tsuzuki, S.; Uchimaru, T.; Mikami, M. *J. Phys. Chem. B* **2009**, *113*, 5617–5621.
(66) Hunt, P. A.; Gould, I. R. *J. Phys. Chem. A* **2006**, *110*, 2269–2282.
(67) Thar, J.; Zahn, S.; Kirchner, B. *J. Phys. Chem. B* **2008**, *112*, 1456–1464.
(68) London, F. *J. Phys. Radium* **1937**, *8*, 397–409.
(69) McWeeny, R. *Phys. Rev.* **1962**, 126.
(70) Ditchfield, R. *Mol. Phys.* **1974**, *27*, 789–807.
(71) Wolinski, K.; Hilton, J. F.; Pulay, P. *J. Am. Chem. Soc.* **1990**, *112*, 8251–8260.
(72) Cheeseman, J. R.; Trucks, G. W.; Keith, T. A.; Frisch, M. J. *J. Chem. Phys.* **1996**, *104*, 5497–5509.
(73) Pepin, M.; Hubert-Roux, M.; Martin, C.; Guillen, F.; Lange, C.; Gouhier, G. *Eur. J. Org. Chem.* **2010**, *2010*, 6366–6371.
(74) Shen, T.; Langan, P.; French, A. D.; Johnson, G. P.; Gnanakaran, S. *J. Am. Chem. Soc.* **2009**, *131*, 14786–14794.
(75) Chundawat, S. P. S; Bellesia, G.; Uppugundla, N.; Sousa, L. C.; Gao, D.; Cheh, A. M.; Agarwal, U. P.; Bianchetti, C. M.; Phillips, G. N.; et al. *J. Am. Chem. Soc.* **2011**, *133*, 11163–11174.